MICROELECTROMECHANICAL INDUCTORS WITH HIGH INDUCTANCE DENSITY VIA MECHANICAL ENERGY STORAGE

Vikram Divakar[*], Yaxing Zhang, Justin C. Zito, Everett A. Salley and David P. Arnold
Interdisciplinary Microsystems Group, Dept. Electrical and Computer Engineering, University of Florida
Gainesville, FL, United States
*Presenting Author: vikramdivakar@ufl.edu

Abstract: This paper reports the design, fabrication and testing of microelectromechanical inductors (MEMIs) that show high electrical inductance by storing energy via a mechanically compliant flexure. The microfabricated MEMI structures comprise a simple electroplated Cu beam that is placed in a static magnetic field. Upon application of ac current, the conductor vibrates via electrodynamic interactions with the magnetic field. This electromechanical behavior manifests as a highly reactive (inductive) one-port electrical impedance. In this work, we explain the microfabrication processes and the subsequent characterization of a variety of test structures, which exhibit a peak quality factor up to 5.6 with net areal inductance densities of up to 3.5 $\mu H/mm^2$. These devices are envisioned as a passive energy storage component for exploring high-power-density electrical power converters.

Keywords: Inductors, electrodynamic transduction, energy storage, passive components, power converters

INTRODUCTION

Inductors are an integral part of power electronic circuits. Nowadays, there is a great effort underway to miniaturize inductors to enable fully integrated single-chip electrical power converters [1-6]. This motivates the need for high-inductance-density and high-Q (efficient) microfabricated inductors with form factors that are amenable for integration or co-packaging with silicon integrated circuits (low profile and small areal footprint).

Most research in this regard is aimed at increasing the inductance densities of microinductors by including high-permeability magnetic core material. For example, Xu et al. employed a soft magnetic CoZrTa thin film ring structures around copper spiral inductors to obtain a Q factor greater than 3 at 1 GHz [6]. At such high frequencies, the hysteretic and eddy current losses from the soft magnetic core lead to limit the efficiency of the inductor [7]. In general it has been difficult to realize magnetic-core based inductors with high inductance density and high quality factor.

The key working principle of the proposed microelectromechanical inductor (MEMI) to achieve high inductance is that mechanical energy storage is used rather than magnetic field energy storage [8]. Mechanical energy storage mechanisms have been shown to possess high energy-density [9].

The device here is an electrically conducting slender beam mechanically supported at each end, as shown in Fig. 1. The device is electrically excited by an external circuit and is set into mechanical oscillation by virtue of a static magnetic field applied perpendicular to the length of the conductor but in plane with the substrate. This results in an electrodynamic actuation, where potential energy is stored via strain, and kinetic energy is stored via inertia of the moving beam. The mechanical energy storage "appears" like inductance due to the electromechanical coupling between the mechanical and electrical energy domains [10]. As will be shown, the apparent electrical inductance of the device can be substantially large, particularly near the mechanical resonance.

This paper is a continuation of the work done by Zhang et al., where proof-of-concept results were demonstrated for macroscale devices [8]. Here, we report the fabrication and testing of *microscale* electromechanical inductors. The microelectro-mechanical inductors explored here operate at "easier-to-implement" kHz frequencies (rather than <100 Hz) and are physically much smaller. These devices are a step toward future development of compact, high-performance power conversion circuitry using these electromechanical energy storage elements.
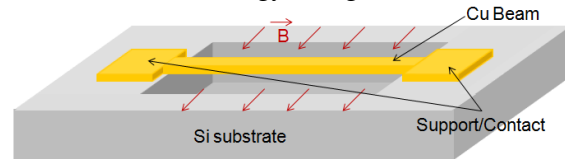

Fig. 1: Microelectromechanical inductor (MEMI) structure

DEVICE MODEL

The physics for the microscale devices remains the same as their macroscale counterparts as discussed by Zhang et al. [8]. The system can be modeled as a lumped system as shown in Fig. 2. The mechanical parameters such as the damping coefficient, equivalent mass, and equivalent spring stiffness are modeled as an resistance, inductance, and capacitance, respectively (b_m, m_m and $C_m=1/k_m$). The electrodynamic transduction is modeled as a gyrator with a gyration ratio denoted by $K=Bl$ (units of $T \cdot m$).

The equivalent one-port circuit representation of the device is also shown in Fig. 2, where the mechanical domain circuit elements have been reflected across the gyrator as equivalent electrical circuit elements. The net electrical behavior appears as

a resistor, inductor, and parallel LRC network all in series. The added inductance K^2/k_m represents the mechanically induced inductance of the system. The reflected resistance and capacitance also play a role in the frequency-dependent apparent impedance.
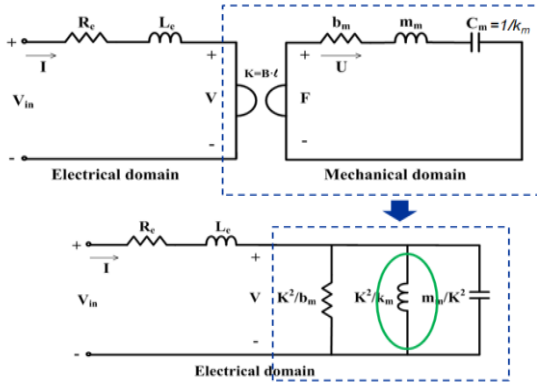

Fig. 2: Lumped element model of the MEMI

FABRICATION

Rectangular cross-section, beam-type MEMI structures are fabricated using silicon microfabrication technology. Fig. 3 illustrates the process steps involved.
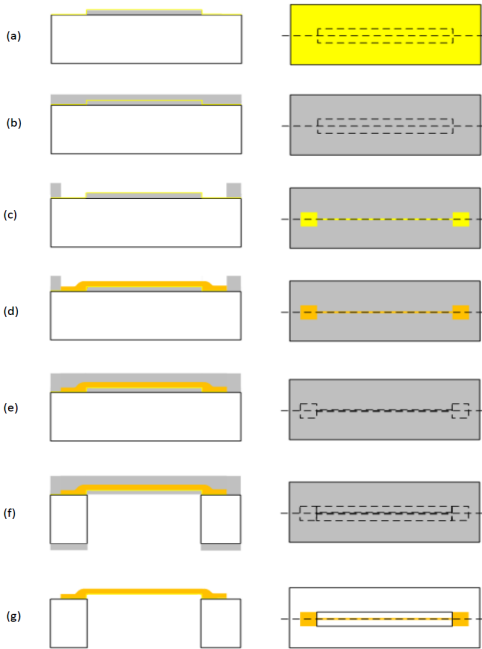

Fig. 3: Microfabrication process for beam-type MEMI structures

The process starts with a standard silicon wafer. A sacrificial photoresist layer (Shipley 1813) is first patterned, followed by sputtering of a Ti/Cu seed layer. The thickness of the Ti layer and the Cu layer are 100 nm and 200 nm respectively. Another photoresist layer (AZ 9260) is then patterned as an electroplating mask to define the conductor geometry. The copper conductor is then electroplated (100 mA DC for 40 minutes). After stripping the photoresist mask, the Cu and Ti seed layers in the non-plated areas are removed by chrome etchant and diluted HF, respectively. Next, a dummy wafer is attached to the top side of the wafer for mechanical support during the subsequent backside silicon etch/beam release process. The backside of the wafer is photolithographically patterned followed by deep reactive ion etch (DRIE), removing the silicon underneath the conductors to release the conductors. The photoresist is then removed by acetone to separate the processed wafer from the dummy wafer.

Two different beam end-supports are explored: clamped supports and "serpentine spring" supports. A variety of clamped-clamped beams are designed with length 3.0–8.4 mm, width 100–800 µm and thickness 5 or 10 µm. The specific dimensions of the beams are given in Table. 1. In addition to straight beams, beams with serpentine spring supports are also fabricated with dimensions shown in Table 2. Adding the serpentine support is expected to increase the mechanical inductance of the MEMI by virtue of lowering the stiffness of the moving structure. Fig. 4 shows the structures fabricated.

Table 1: Parameter variations of MEMI prototypes dimensions (clamped support)

Dimension	Value
Length	3 / 5.7 / 8.4 mm
Width	100 / 200 / 300 / 400 / 500 / 600 / 700 / 800 µm
Thickness	5 / 10 µm

Table 2: Parameter variations of MEMI prototypes dimensions (serpentine spring support)

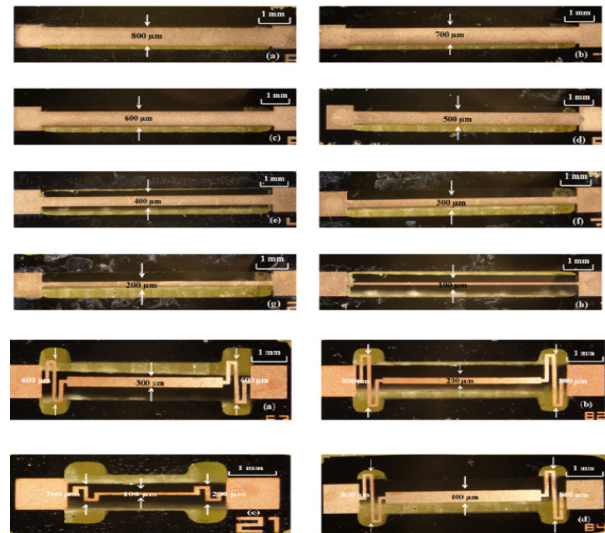| Dimension	Value
Length	1.6 / 4.3 mm
Width	100 / 200 / 300 / 400 µm
Thickness	5 / 10 µm
Serpentine width	200 / 400 / 600 / 800 µm
Serpentine line-width	100 µm

Fig. 4: Microfabricated MEMI structures showing clamped and serpentine spring supports

EXPERIMENTAL RESULTS

The microfabricated devices are tested by measuring the complex impedance over a 8 kHz bandwidth using an HP 4294A impedance analyzer with four needle probe contacts under a current excitation of 200 µA.

For testing, two different assemblies of external permanent magnets (NdFeB) were used to provide the magnetic field. First six permanent magnets were arranged in a Halbach configuration to generate a uniform magnetic field of 0.6 T (Fig. 5(a)). The second, shown in Fig. 5(b), uses two magnets placed underneath the MEMI structure, offering a smaller footprint (144 mm^2) and higher (but less uniform) average magnetic field (0.7 T). The microstructures were first tested with the uniform field of the Halbach configuration. The best performers were then subsequently tested using the smaller, two-magnetic assembly.
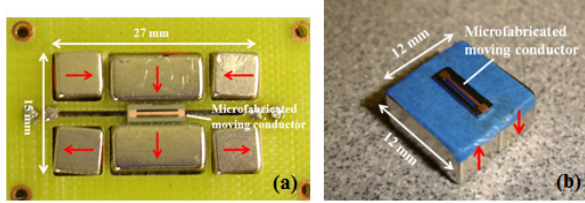

Fig. 5 Permanent magnet setup (a) 6-magnet Halbach array (b) 2-magnet array.

An example impedance plot is shown in Fig. 6, expressed as L and Q, where $Q = \omega L / R$ and $\omega = 2\pi f$ *rad/s*. For the purposes of this paper, the parameter of interest is the maximum electrical quality factor (Q_{max}) and the inductance (L_{Qmax}) at that frequency (f_{Qmax}). These data enable comparison between different designs.
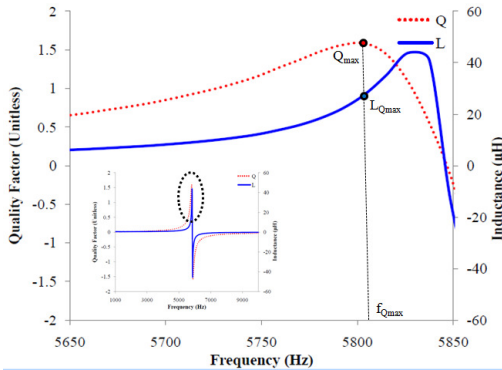

Fig. 6: Example plot of impedance data obtained from the setup

Fig. 7 and Fig. 8 shows scatter plots of the inductance and the peak quality factors vs. frequency of occurrence (f_{Qmax}) for 5-µm-thick and 10-µm-thick beams, when tested with the Halbach array. From the test results, we can make the following summarizations. First, comparing just the clamped-clamped (blue) vs. serpentine structures (red), it is

clear that the serpentine structures indeed have higher inductance and lower operating frequencies. In general, however, the clamped-clamped structures achieved higher quality factors. Considering trends with frequency, the inductance (L_{Qmax}) decreases as the frequency (f_{Qmax}) increases for both the clamped-clamped prototypes and serpentine-spring-supported prototypes.
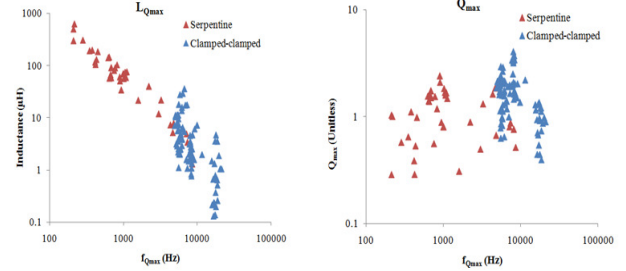

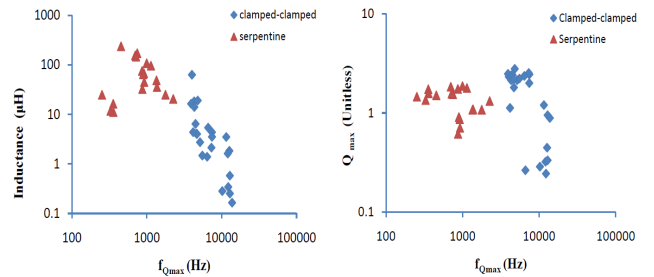*Fig. 7: Scatter plots (a) L_{Qmax} vs f_{Qmax} (b) Q_{max} vs f_{Qmax} for 5 µm thick beams*

Fig. 8: Scatter plots (a) L_{Qmax} vs f_{Qmax} (b) Q_{max} vs f_{Qmax} for 10 µm thick beams

Table 3 summarizes the best results for the various prototypes when tested with the 2-magnet assembly. Prototype 1 with 5.7 mm length, 400 µm width, and 10 µm thickness yields a maximum quality factor of 4.1 and an inductance of 1.7 µH at 8076 Hz. Considering the footprint of the magnetic array, this inductance corresponds to an areal inductance density of 3.5 µH/mm^2. Prototype 5 with 4.3 mm length, 400 µm width, and 5 µm thickness connected with two serpentine springs with 100 µm line width and 600 µm spring width yields an inductance of 502 µH and a maximum quality factor of 1.0 at 212 Hz.

Table 3: Prototype test results summary

Device #	1	2	3	4	5	6	7	8
Length (mm)	5.7	5.7	5.7	5.7	4.3	4.3	4.3	4.3
Width (µm)	400	400	300	300	400	400	400	300
Thickness (µm)	10	10	10	10	5	5	5	5
Serpentine width (µm)	N/A	N/A	N/A	N/A	800	600	800	600
f_{Qmax} (kHz)	8.07	8.11	8.05	7.77	212	626	674	902
L_{qmax} (µH)	1.74	1.68	3.24	3.15	501.94	141.43	66.98	50.96
Q_{max}	4.06	3.66	3.31	3.39	1.04	1.57	1.6	2.12

From the lumped element model of the device we understand that the apparent inductance boost is given by the K^2/k_m term where $K = Bl$ (T·m). Theoretically, by applying a higher magnetic field, inductance increases exponentially. To verify this behavior, MEMI structures were placed in the center of a dc electromagnet (GMW magnet systems, model 3473-70) (Fig. 9). The magnetic field was stepped from 0.3 T to 2.0 T, and the impedance was measured at each value of the applied magnetic field. Comparison plots of inductance vs frequency and Q vs frequency at various fields for an 8400 μm x 200 μm x 10 μm clamped-clamped beam are shown in Figs. 10 and Fig. 11 respectively. A high Q of 5.56 and an inductance of 68 μH at 4.53 kHz was noted for the same.
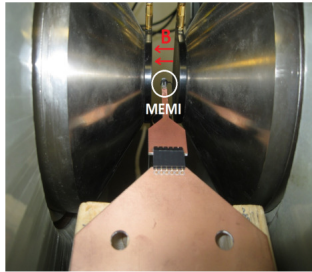

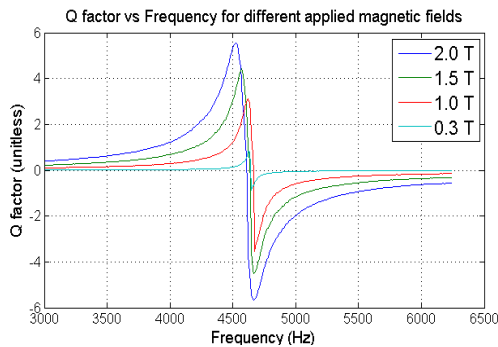*Fig. 9: Setup for testing the MEMI in a variable field electromagnet*

Fig. 10: Q factor vs frequency for 8400-200-10 clamped-clamped beam at various magnetic fields
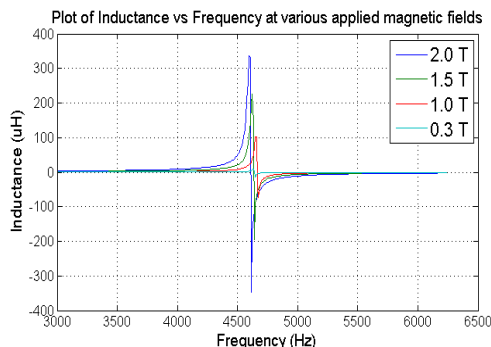

Fig. 11: Inductance vs frequency for 8400-200-10 clamped-clamped beam at various magnetic fields

CONCLUSION

In this paper, the concept of implementing high-inductance-density microelectromechanical inductors is realized. The concept involves storing energy in the mechanical domain rather than in the magnetic core of a conventional inductor. Devices of different geometries and operation are microfabricated and tested with an inductance density up to 3.5 μH/mm^2. Devices tested in a 2.0 T magnetic field showed a maximum Q factor of 5.56. Though the maximum Q-factor of MEMI devices is less than the conventional microfabricated inductors, high inductance densities of the devices are quite promising towards the development of chip scale microinductors.

The quality factor may be improved by careful design optimization and/or by fabricating the beams with high relative permeability ferromagnetic materials to enhance the magnetic field acting on the beam. The ultimate vision is to be fabricate devices with permanent micromagnets [11] embedded in the substrate directly, to enable fully microfabricated, self-contained devices.

It should be noted that these MEMI structures are not true inductors. They exhibit the strong inductance and quality factor over a narrow frequency band. Because of this, the devices may require specific or new types or power converter architectures.

REFERENCES

[1]   Takamiya M, Onizuka K, Ishida K,Sakurai T 2010 DC-DC Converter Technologies for On-Chip Distributed Power Supply Systems - 3D Stacking and Hybrid Operation Springer, 221-247

[2]   Wens M and Steyaert M 2009 An 800mW Fully-integrated 130nm CMOS DC-DC Step-down Multi-phase Converter, With On-chip Spiral Inductors and Capacitors *ECCE 2009. IEEE* , 3706-3709

[3]   Wibben J and Harjani R 2008 A High-Efficiency DC-DC Converter Using 2nH Integrated Inductors IEEE J. Solid-State Circuits, **43**, 844-54

[4]   Meere R, O'Donnell T, Bergveld H J, Wang N, O'Mathuna S C 2009 Analysis of Microinductor Performance in a 20-100 MHz DC/DC Converter IEEE Trans. Power Electron. **24** 2212-8

[5]   Flynn D, Desmulliez M P Y 2009 Design methodology and fabrication process of a microinductor for the next generation of DC–DC power converters. *Microsyst. Technol.* 15, 8 , 1233-1243

[6]   Xu W, Wu H, Gardner D S, Sinha S, Dastagir T, Bakkaloglu B, Cao Y, Yu H 2011 Sub-100 μm scale on-chip inductors with CoZrTa for GHz applications Journal of Applied Physics **109** 07A316

[7]   Gardner D S, Schrom G, Paillet F, Jamieson B, Karnik T, Borkar S 2009 Review of On-Chip Inductor Structures With Magnetic Films IEEE Trans. Magn. **45** 4760-6

[8]   Zhang Y, Arnold D P, Electromechanical Inductors for Power Converter Applications *Proceedings Power MEMS, 2010* 131-134

[9]   Hill F, Havel T, Hart A J, Livermore C 2008 Storing Elastic Energy in Carbon Nanotubes *PowerMEMS 2008 (Sendai, Japan, 9-12 November 2008)* 35–38

[10] Cheng S, Wang N, Arnold D P 2007 Modeling of magnetic vibrational energy harvesters using equivalent circuit representations J. Micromech. Microeng. 17 S2328

[11] Arnold D P and Wang N 2009 Permanent Magnets for MEMS J. Micromech. Microeng. 18 S1255